

3rd International Workshop on High-Order CFD Methods

January 3-4, 2015 Kissimmee, USA

Abstract for the Onera NXO method

on case 2.3 : **Heaving and Pitching Airfoil**

Jean-Marie Le Gouez¹

*CFD and Aeroacoustics Department,
Onera - The French Aerospace Lab,
F- 92322 Châtillon France*

1 Code description

Discretization by cell-centered Finite Volume Method, 1 dof / eqn / cell.

Upwind-biased convective scheme based on characteristic splitting of the conservative variables extrapolated at the cell interface (“state-upwind” scheme)..

Evaluation of left and right conservative variables as surface averages on the interface interpolated from the volume averaged conservative variables inside cells. The interpolations are based on weighted least-square polynomial reconstructions inside partially biased stencils (collection of cells centered on the left, respectively right cell on either side of the interface).

Centered scheme for the evaluation of gradients for the diffusive fluxes,

Evaluation of centered conservative variables gradients as surface averages on the interface based on a weighted least-square polynomial reconstruction inside a face-centered stencil (union of the 2 stencils used for the convective operator).

These reconstructions are done in the pre-processor and provide sets of linear interpolation coefficients for the conservative variables fields and their gradients, from cell-averaged to surface-averaged quantities.

The degree of the reconstructed polynomial is the highest enabled by the number of cells in the stencil (number of monomials *1.5), depending on the successive neighbours insertion (ref 1.).

Relevant solvers

Time accurate solutions either

- Non-linear implicit by dual time-stepping (Explicit RK for pseudo-time inner iterations), or
- Explicit Runge-Kutta options from 3 to 6 stages.

Non-linear implicit by dual time-stepping was used for this test-case, with RK 4 stages, CFL 3 for the dual local time stepping iteration.

The real-time step is set to $1/160^{\text{th}}$ or $1/320^{\text{th}}$ of the flapping time, 300 to 500 local pseudo-time-stepping iterations are performed in each time step. The choice of this rather high time step is due to the long computation of the metrics and coefficients of the space scheme at each new position of the deforming grid.

ALE fully conservative formulation for the grid motion / deformation with cell metrics Jacobians varying function of time.

Boundary conditions :

- outside boundary managed by Riemann invariants in the normal direction to the face, reference flow conditions are at rest.
- no-slip boundary : reduced stencil size and degree of reconstruction from k5 or k4 inside the field → k3.

High-order capability

k-exact reconstruction coded and verified up to a 6th degree full base of monomials.

¹ jean-marie.le_gouez@onera.fr, AIAA member.

Computations done on grids made of linear elements (triangles), with one single flux evaluation per equation on each interface.

Parallel capability

- Loop-based Open-MP programming.
For the runs of this test-case 2.3, an acceleration between 25 and 28 was recorded, on a 8-socket SGI UV board (8 Nehalem processors, 32 cores, 32 OMP threads) with respect to a single Nehalem core.

Post-processing

- Output in TecPlot™ Format.
- Internal binary format for visualizations inside the GUI.

2. Case summary

Machines used (number of cores if parallel) : 8-Nehalem SGI-UV, 32 cores, 32 OMP threads activated

Tau-bench wall clock times (sequential) on machines used : 9.4s.

The Work load (in Tau_bench Work units) are computed as the wall clock time multiplied by 32, divided by the Tau-Bench wall clock time (sequential).

3. Meshes

Description of meshes used for the case.

Grids generated by gmsh, grid topology and element connectivity fixed in time.

Grid deformation at each time step and node velocity computed by analytical functions.

$$\vec{X}(t) = \vec{X}_0 + \varphi(d)M_\theta(\vec{X}_0 - \vec{X}_c) - U_\infty t\vec{e}_x + a \sin \varpi t \vec{e}_y$$

$$\vec{W}(t) = -\varphi(d)\varpi \sin \varpi t \Omega_0 \vec{e}_z \wedge (\vec{X}_0 - \vec{X}_c) - U_\infty \vec{e}_x + a\varpi \cos \varpi t \vec{e}_y$$

with M_θ the matrix of rotation of angle θ , $W(t)$ the grid nodes velocity, $\varphi(d)$ a blending function of the distance d from each node to the wing, equal to 1 for $d=0$ and to 0 for $d=-5c$, (c the wing chord), \vec{X}_0 the reference position of the node in the non perturbed grid, \vec{X}_c the reference position of the centre of rotation.

The computation is done in the absolute reference frame with fluid at rest at infinity, the free stream velocity $U_\infty \vec{e}_x$ is transferred in the grid motion and in the moving wall boundary condition.

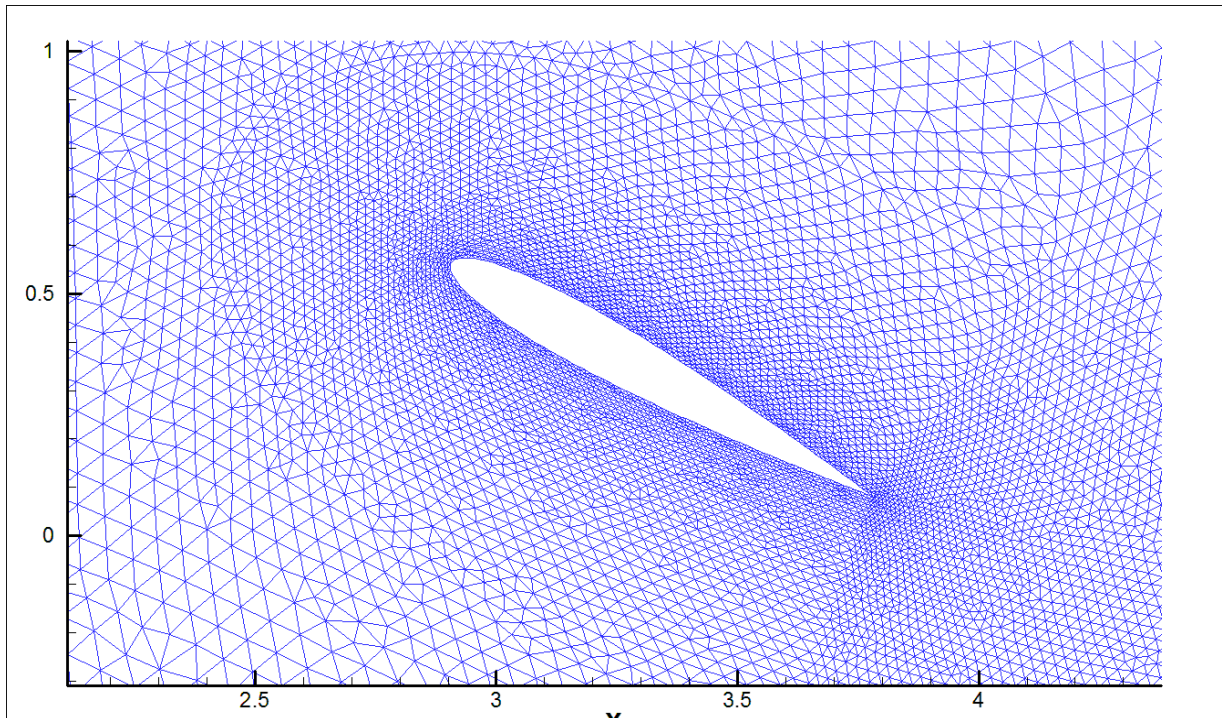


Figure 1a : Tilted and deformed mesh
(from gmsh, frontal meshing by triangles, normal shrinking 0.33, hwall=c/71)

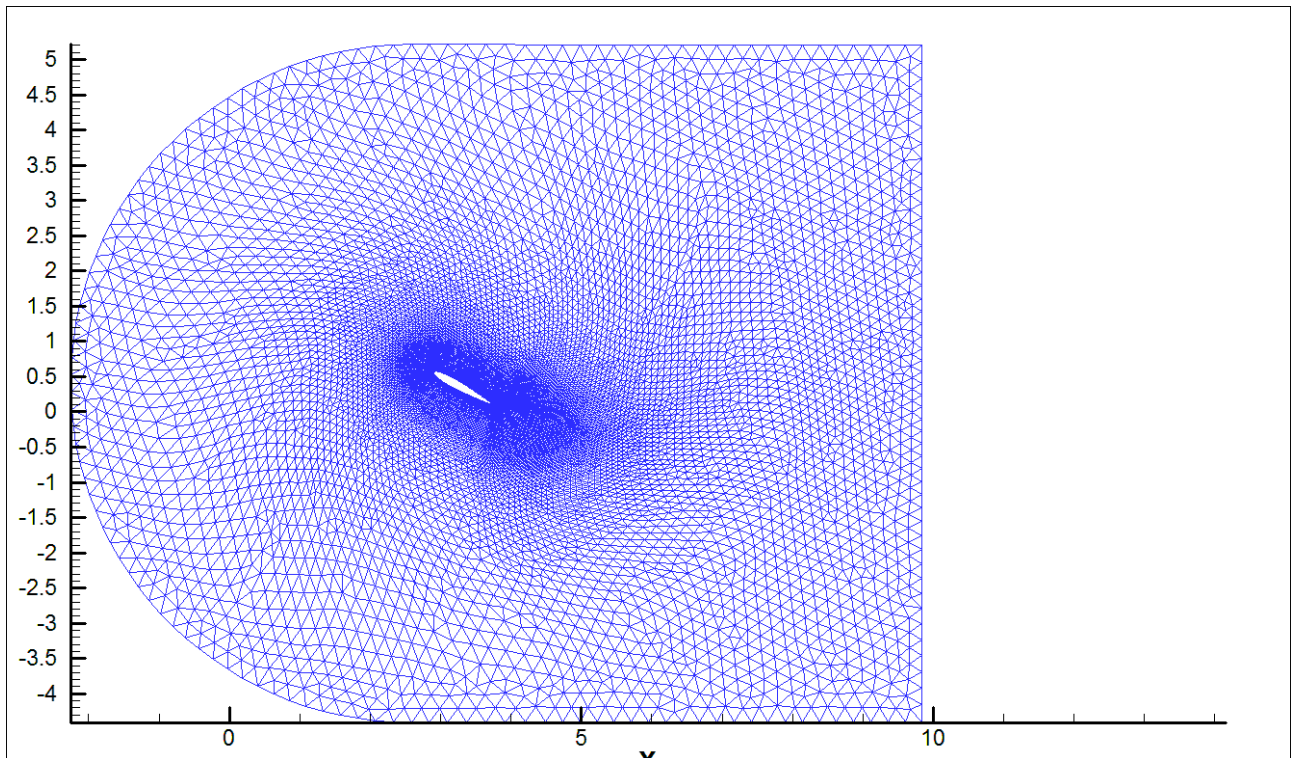


Figure 1b : Full view of the grid 3, external boundary only in translation

Grid characteristics : 5 grids were used, with a reference cell size = $c/17, c/25, c/35, c/50, c/71$ (ratio of $\sqrt{2}$ between 2 successive grids). Wall cell size = $0.5 * \text{ref cell size}$.

The gmsh grid made of isotropic triangles is shrunk in the normal direction by a factor 3 next to the wall (this factor decreases towards the outer boundary)

Same grid size expansion to the outer boundary.

Grd1 : href = $c/17$, h wall = $c/35$, outer boundary at 6 chords, ncells = 6138

Grd2 : href = $c/35$, h wall = $c/50$, outer boundary at 6 chords, ncells = 12119

Grd3 : href = $c/50$, h wall = $c/71$, outer boundary at 6 chords, ncells = 24639

Grd4 : href = $c/71$, h wall = $c/100$, outer boundary at 6 chords, ncells = 48720

Grd5 : href = $c/100$, h wall = $c/142$, outer boundary at 6 chords, ncells = 90429

Domain size: Outer boundary 6 to 80 chords away in all directions. A check was made to verify that the solution (time integral of the fluid/wing force and power) were only slightly influenced by the distance to the outer boundary.

Final results were recorded for the smaller extent grids grd1 to grd5 (6 chords).

A large distance is necessary to obtain a good accuracy on the drag in steady flow configurations, while a shorter distance is sufficient for the unsteady perturbation to be mostly contained within the grid (acoustics perturbations only travel 5 chords during the flapping motion).

Physical simulation time : 1.5 flapping time.

Time steps : 160 or 320 physical time steps flapping time, 300 to 500 pseudo-time iterations per time step.

4. Results

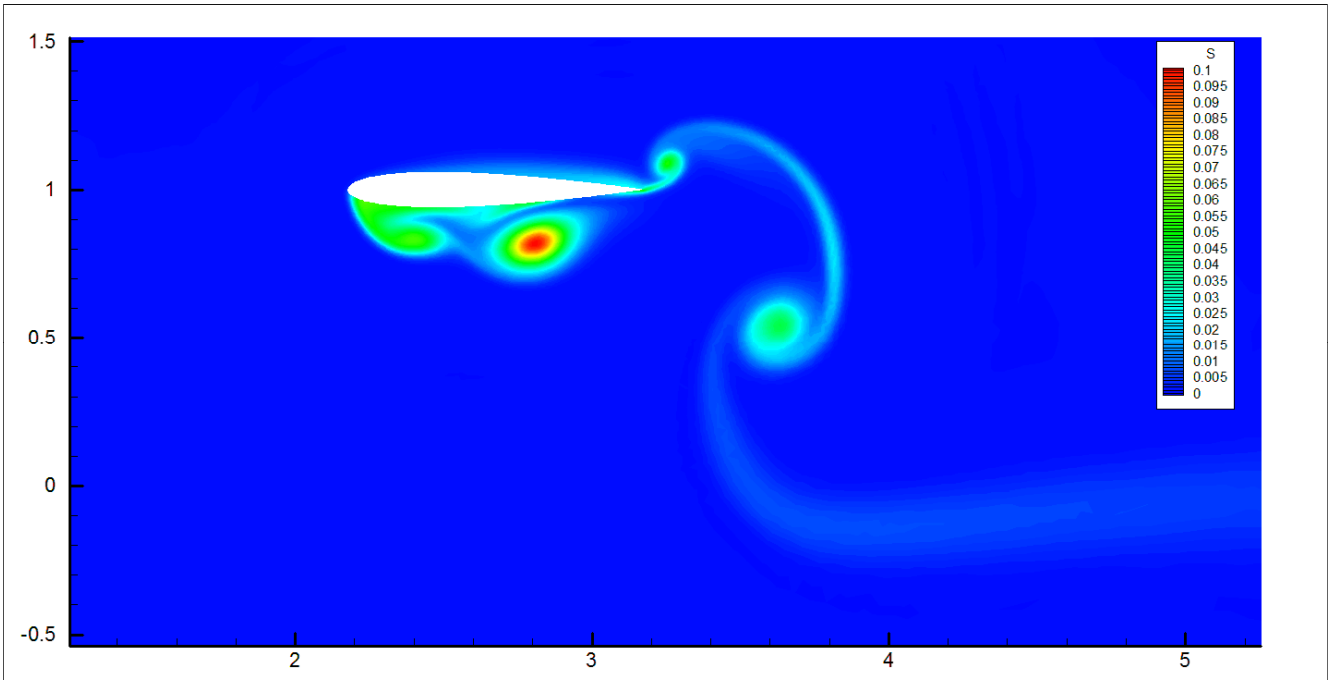
CPU usage :

Run example : finer grid (grd4, 48 720 triangles).

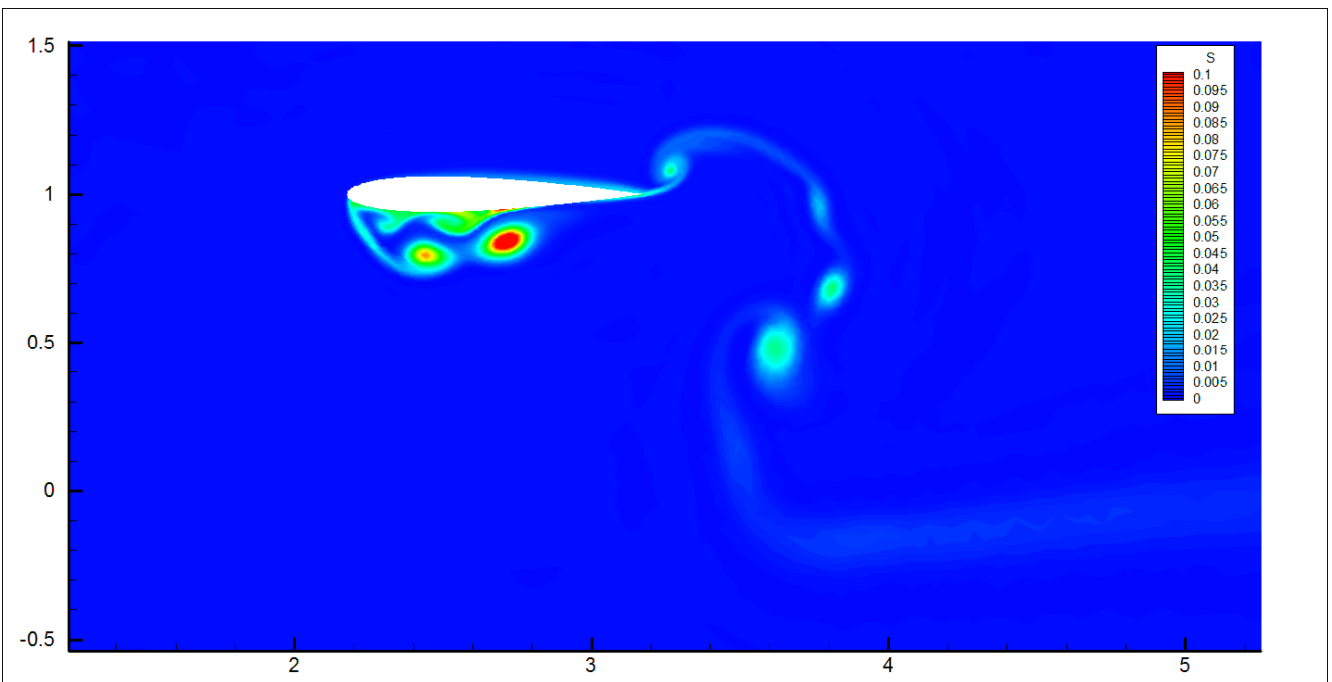
For 1 time unit (flapping time), 320 physical time steps → Wall clock time = 11740s = 3h 16mn

Cpu Work = $11740 * 32 / 9.4 = 39\,965$ W.U.

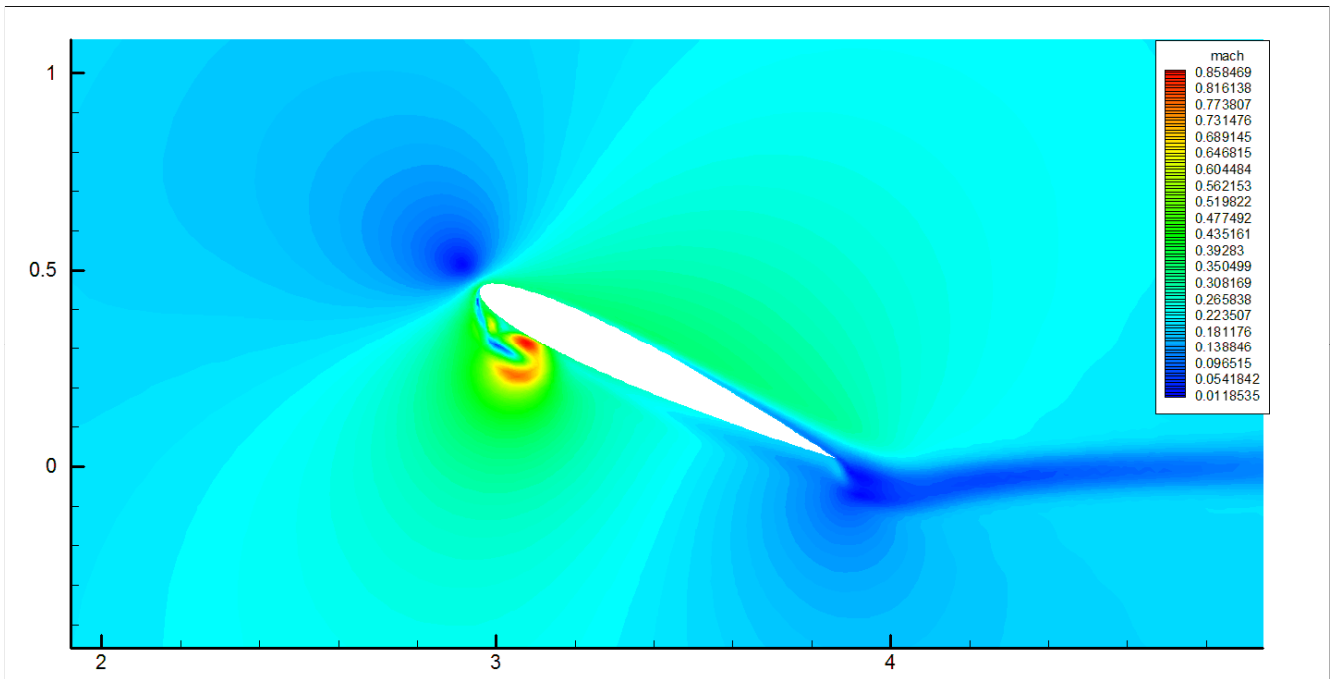
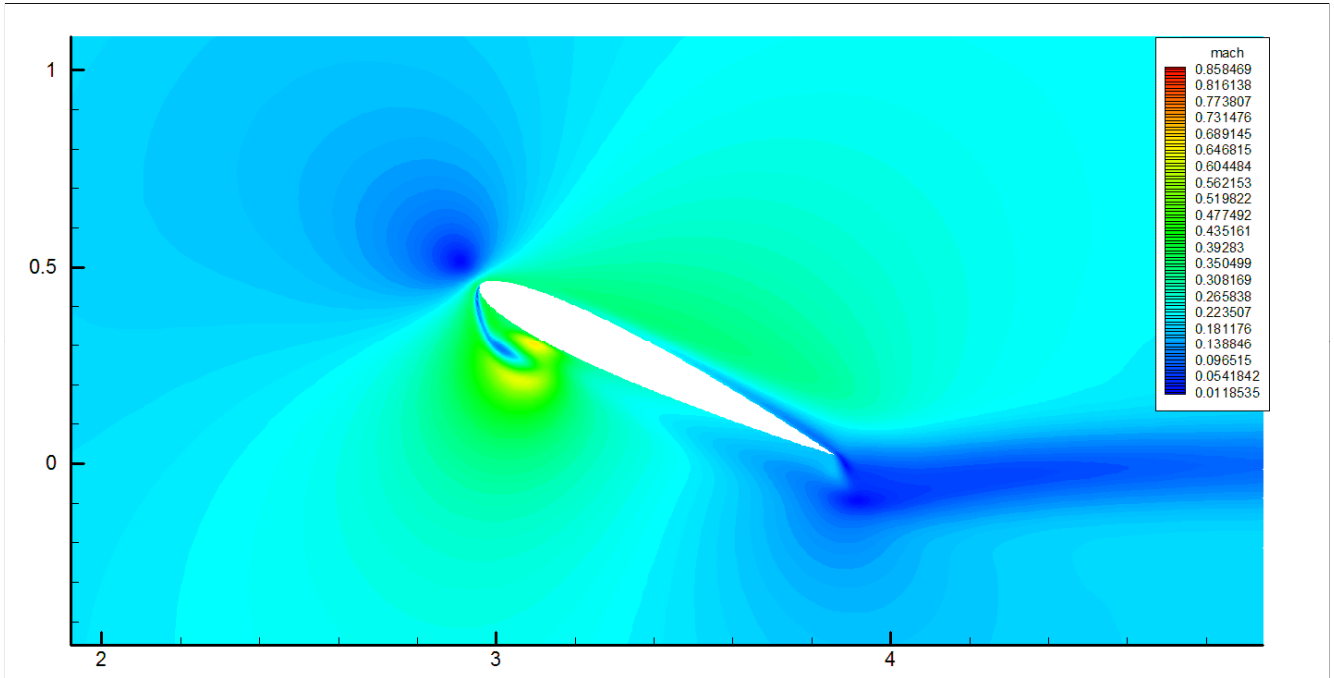
A much more stable wake is computed for Reynolds = 1000 than for Reynolds = 5000.
Mach 1 is reached in the recirculation bubble at the middle of the ascending phase for Reynolds = 5000.



End of the flapping motion, Reynolds = 1000, entropy



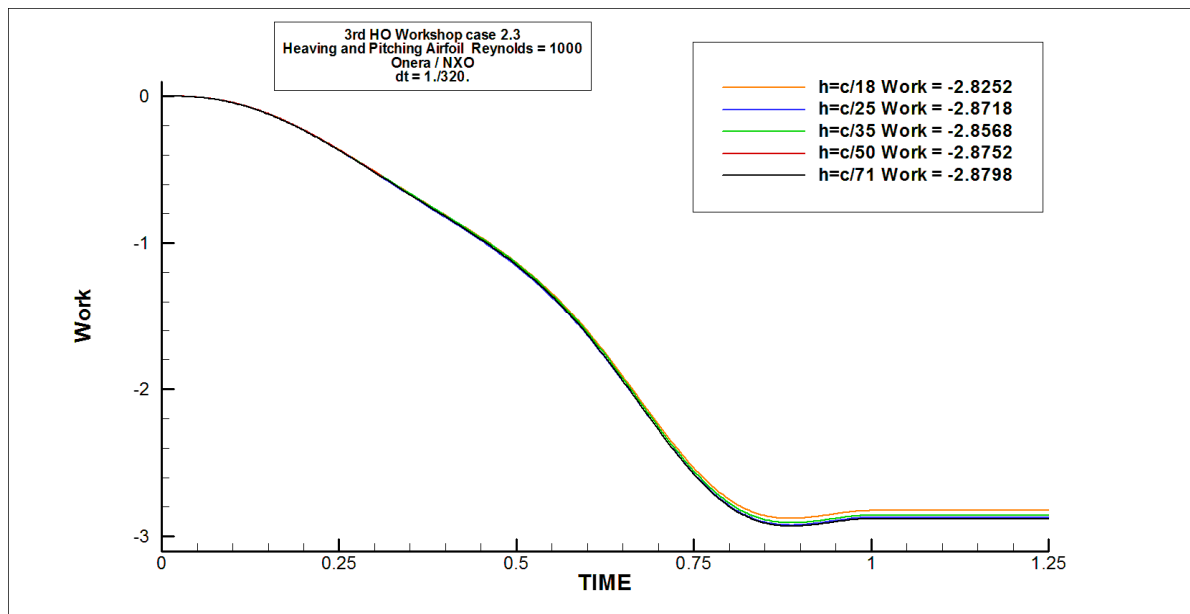
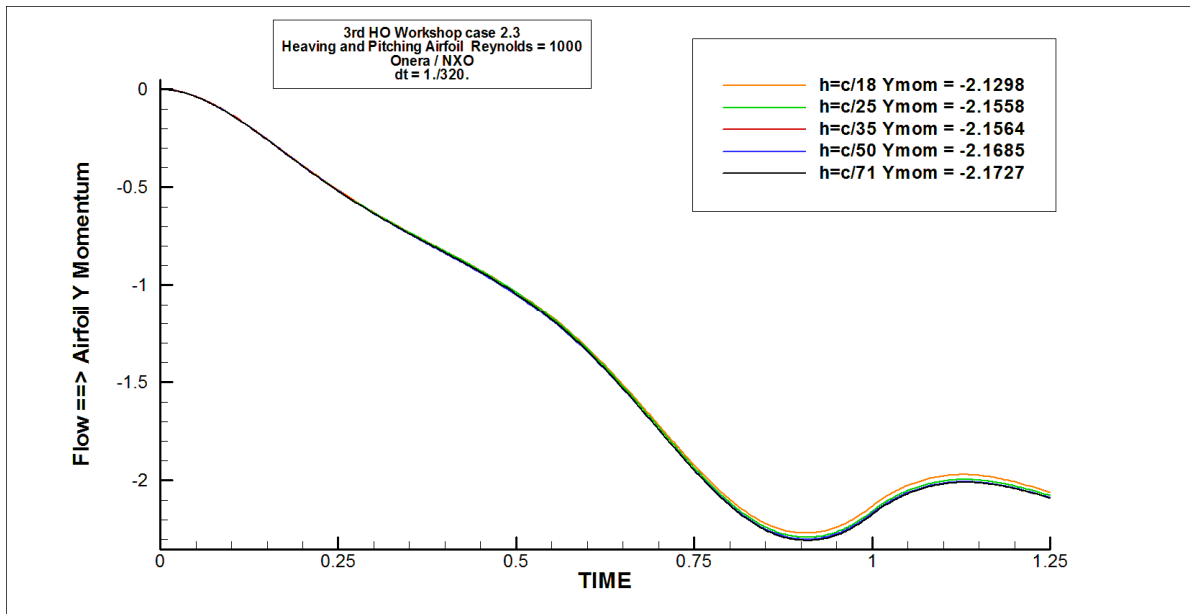
End of the flapping motion, Reynolds = 5000, entropy

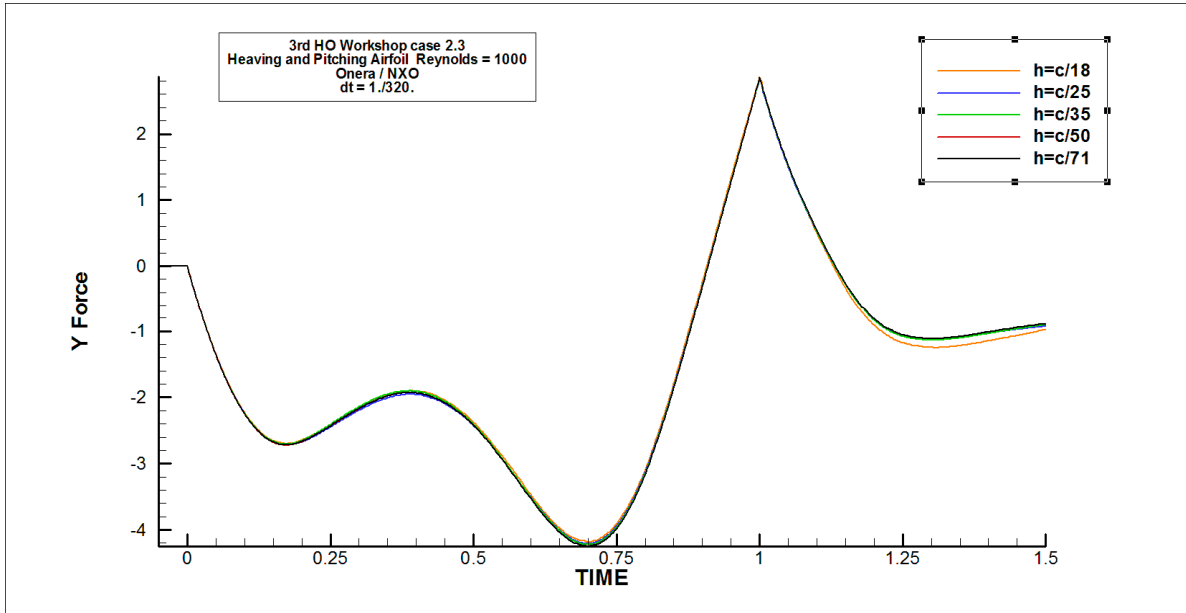


Results for Reynolds = 1000

For the work and the Y-momentum to the wing, are shown the relative discrepancy with respect to the finest grid results.

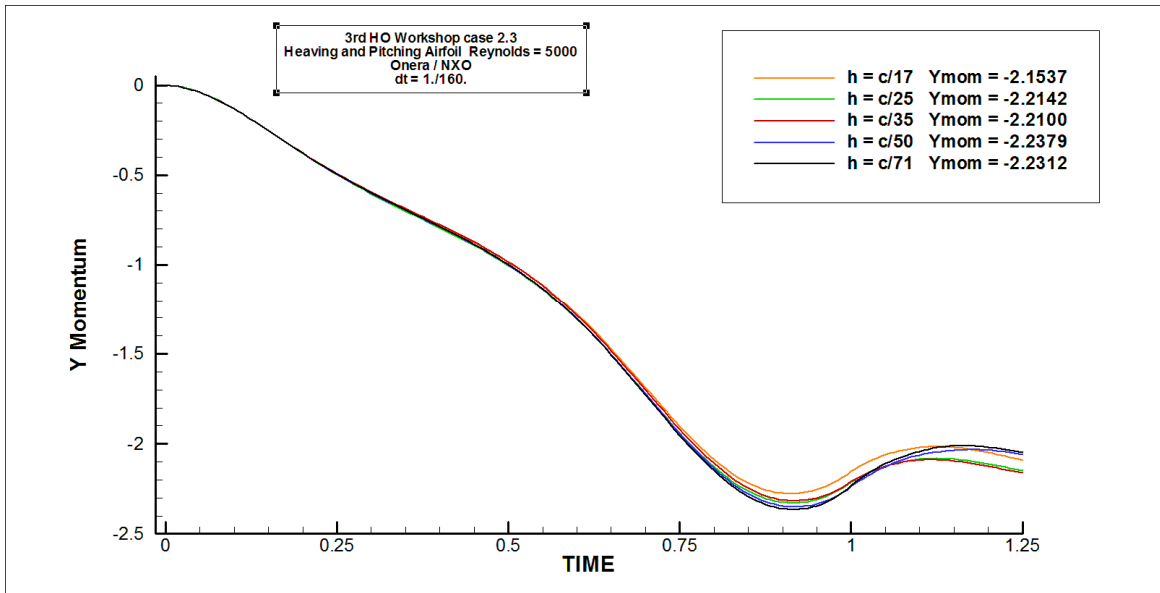
	Wall cell size	Ndof/eqn	Y-momentum	Work
Grd1	c/35	6138	-2.1298 (2.e-2)	-2.8252 (1.9e-2)
Grd2	c/50	12119	-2.1658 (3.2e-3)	-2.8718 (2.8e-3)
Grd3	c/71	24639	-2.1564 (7.5e-3)	-2.8568 (8.e-3)
Grd4	c/100	48720	-2.1685 (1.9e-3)	-2.8752 (1.6e-3)
Grd5	c/140	90429	-2.1727 (0)	-2.8798 (0)

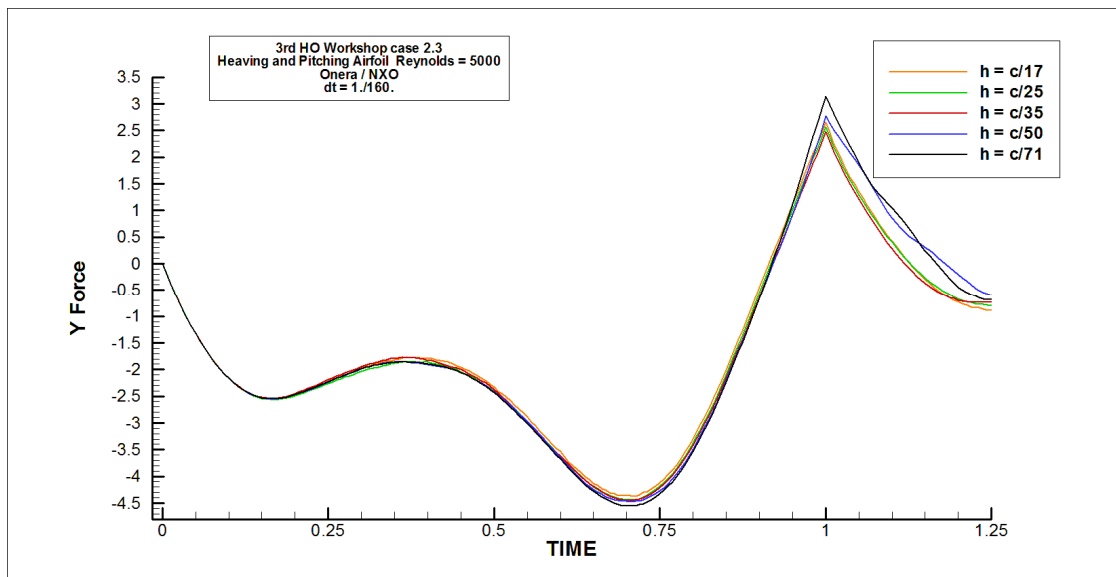
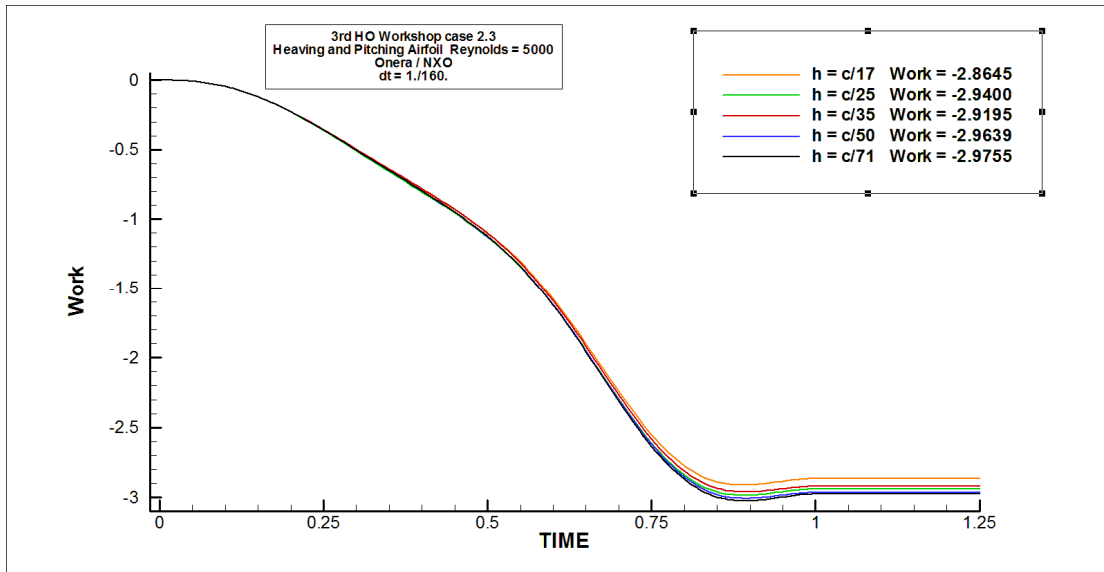




Results for Reynolds = 5000

	Wall cell size	Ndof/eqn	Y-momentum	Work
Grd1	c/35	6138	-2.1537 (3.5e-2)	-2.8645 (3.7e-2)
Grd2	c/50	12119	-2.2142 (7.6e-3)	-2.9400 (1.2e-2)
Grd3	c/71	24639	-2.2100 (9.5e-3)	-2.9195 (1.9e-2)
Grd4	c/100	48720	-2.2379 (3.0e-3)	-2.9639 (3.9e-3)
Grd5	c/140	90429	-2.2312 (0)	-2.9755 (0)



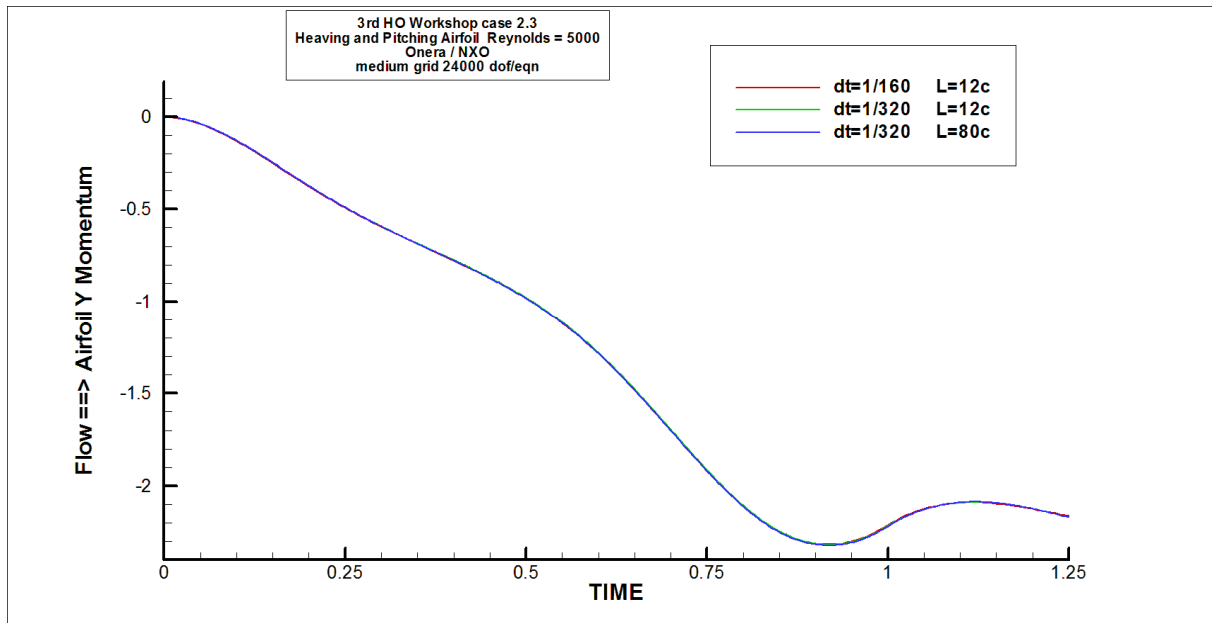


The convergence with the mesh size is not monotonic, the results on grid2 are better than would be expected in extrapolating from the solutions on the finer grids.

In fact, the solution on the finer grids exhibit more flow features, especially for the higher Reynolds number, like vortex stretching or vortex pairings (mostly after the end of the flapping motion), which explains a lower convergence index for this higher Reynolds number flow simulation.

Complement: Verification of the sensitivity of the solution to the time step and the distance to the far-field boundary.

This was checked by runs on the medium grid, 24000 cells, with different time steps and distance to the far-field boundary. The momentum transfer from the flow to the wing is essentially unaffected.



Reference : **J.-M. Le Gouez, V. Couaillier, F. Renac**

High Order Interpolation Methods and Related URANS Schemes on Composite Grids.

48th AIAA Aerospace Sciences Meeting -Orlando, -USA (04-07 Jan 2010), AIAA-2010-513

External link : Animation of the flow field at Reynolds 5000

http://elsa.onera.fr/Cassiopee/Storage/naca12_pitch3_Re5000_s.avi

http://elsa.onera.fr/Cassiopee/Storage/naca12_pitch5_Re5000_s.avi